Surfactant−Surfactant Molecular Interactions in Mixed Monolayers at a Highly Hydrophobic Solid/Aqueous Solution Interface and Their Relationship to Enhanced Spreading on the Solid Substrate

Qiong Zhou, Yongfu Wu, and Milton J. Rosen*

Surfactant Research Institute, Brooklyn College of City University of New York, Brooklyn, New York 11210

Received April 14, 2003. In Final Form: July 1, 2003

Spreading of mixed aqueous hydrocarbon-chain surfactant solutions on the solid polyethylene (PE) surface has been studied. Synergistic effect on the spreading of the mixed surfactant solution on the PE film has been observed, and the obtained spreading is comparable to superspreading normally obtainable from trisiloxane-based surfactants. Some other interfacial phenomena related to surfactant spreading, such as surfactant−surfactant molecular interactions in the mixtures adsorbed at various interfaces, dynamic contact angle change of the mixed surfactant solutions during the process of spreading on the hydrophobic PE substrate, and surfactant adsorption at the solid/liquid and air/liquid interfaces have been investigated. It is suggested that stronger surfactant−surfactant attractive interactions and greater adsorption at the PE powder/aqueous solution interface than at the air/aqueous solution interface account for the observed spreading enhancement in the mixed hydrocarbon-chain surfactant systems, which is also accompanied by lower dynamic contact angles, implying greater dynamic spreading coefficients.

Introduction

The wetting of a solid surface by liquids plays a critical role in many natural processes and commercial technologies, such as coatings,[1] cosmetics,[2] agrochemicals,[3] the oil industry,[4] textiles,[5] and many others.[6] During the past decade, spreading of surfactant solutions over solid surfaces has attracted considerable interest both in the academic world and in industry, because of its theoretical and practical applications.[7−13] When a liquid spreads on a solid surface, a precursor film of molecular thickness is formed at the spreading edge.[14] The surface tension gradient at this spreading edge of the drop is thought to be the driving force for the spreading. A simple scheme of surfactant solution spreading on purified polyethylene (PE) film is shown in Figure 1. As the spreading front stretches, the concentration of the solution in the precursor film decreases because of the adsorption of surfactant at the solid/aqueous solution interface. Consequently, the surface tension increases at the front relative to the top of the droplet, thereby establishing a surface tension gradient. The faster and greater the adsorption at the solid/aqueous solution interface, the sharper the gradient, and the faster the spreading.

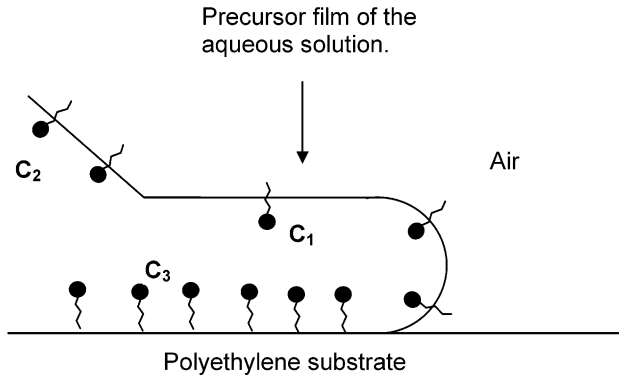

Figure 1. Precursor film of aqueous surfactant solution on PE substrate, with surfactant concentration gradient $C_1 < C_2 < C_3$ at the interfaces, due to the greater adsorption of the surfactant at the solid/liquid than that at air/liquid interface.

The spreading coefficient at the solid/liquid interface ($S_{L/S}$) is quantitatively defined as[15a] $S_{L/S} = \gamma_{SA} - (\gamma_{SL} + \gamma_{LA})$, where γ_{SA} is the interfacial tension of the solid substrate with liquid-saturated air above it, γ_{SL} is the interfacial tension at the solid substrate/liquid interface, and γ_{LA} is the surface tension of the liquid. The quantity $\gamma_{SA} - (\gamma_{SL} + \gamma_{LA})$ is a measure of the driving force behind the spreading process. A negative spreading coefficient indicates that spreading over the solid surface is not energetically favorable. A positive spreading coefficient indicates that the spreading process can occur spontane-

(1) Adams, J. W. In *Surface Phenomena and Additives in Water-Based Coatings and Printing Technology*; Sharma, M. K., Ed.; Plenum Press: New York, 1991; p 23.
(2) Vick, S. C. *Soap, Cosmet., Chem. Spec.* **1984**, May, 36.
(3) Stevens, P. J. G. *Pestic. Sci.* **1993**, *38*, 103.
(4) Callaghan, I. C. In *Defoaming, Theory and Industrial Applications*; Garrett, P. R., Ed.; Surfactant Sci. Ser. 45; Marcel Dekker: New York, 1993; p 119.
(5) Sabia, A. J. *Am. Dyest. Rep.* **1982**, May, 45.
(6) Rosen, M. J.; Dahanayake, M. *Industrial Utilization of Surfactants: Principles and Practice*; AOCS Press: Champaign, IL, 2001.
(7) Ananthapadmanabhan, K. P.; Goddard, E. D.; Chandar, P. *Colloids Surf.* **1990**, *44*, 281.
(8) Tiberg, F.; Cazabat, A. M. *Langmuir* **1994**, *10*, 2301.
(9) Zhu, S.; Miller, W. G.; Scriven, L. E.; Davis, H. T. *Colloids Surf., A* **1994**, *90*, 63.
(10) Stoebe, T.; Lin, Z.; Hill, R. M.; Ward, M. D.; Davis, H. T. *Langmuir* **1996**, *12*, 337.
(11) Svitova, T.; Hoffmann, H.; Hill, R. M. *Langmuir* **1996**, *12*, 1712.
(12) Stoebe, T.; Lin, Z.; Hill, R. M.; Ward, M. D.; Davis, H. T. *Langmuir* **1997**, *13*, 7270.
(13) Nikolov, A. D.; Wasan, D. T.; Chengara, A.; Koczo, K.; Policello, G. A.; Kolossvary, I. *Adv. Colloid Interface Sci.* **2002**, *96*, 325.
(14) Cazabat, A. M.; Valignat, M. P.; Villette, S.; Coninck, J. D.; Louche, F. *Langmuir* **1997**, *13*, 4754.
(15) (a) Rosen, M. J. *Surfactants and Interfacial Phenomena*, 2nd ed.; Wiley-Interscience: New York, 1989; p 242. (b) Rosen, M. J. *Surfactants and Interfacial Phenomena*, 2nd ed.; Wiley-Interscience: New York, 1989; p 394.

10.1021/la030157f CCC: $25.00
Published on Web 08/12/2003

Scheme 1. (A) Surfactant Structures and (B) Stabilization of the Ionic-like Structure of Pyrrolidone in High Ionic Strength Medium

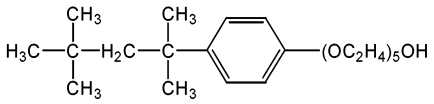

CA-520

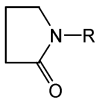

R: n-C_8H_{17}-, C8P
R: n-$C_{12}H_{25}$-, C12P

A

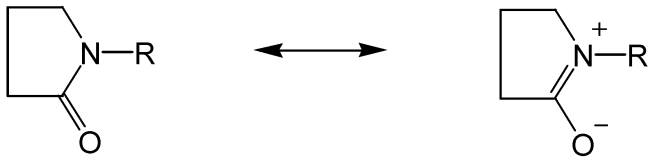

nonionic structure, in low ionic strength medium.

zwitterionic structure, in high ionic strength medium.

B

ously. Furthermore, it is expected that the more positive the spreading coefficient, the greater the spreading area made by the liquid over the substrate. Surfactants can promote spreading by adsorbing at the air/liquid and/or solid/liquid interfaces to reduce γ_{LA} and/or γ_{SL}, making $S_{L/S}$ more positive. Since spreading is a dynamic process, it is possible that the value of the spreading coefficient, $S_{L/S}$, will not be a constant during the process of spreading of the solution.

Previous work in our laboratory[16] has shown that the superspreading enhancement of aqueous solutions on a highly hydrophobic solid substrate by mixtures of a trisiloxane-based surfactant and *N*-alkyl pyrrolidones corresponds to stronger molecular interaction at the solid/aqueous solution interface than molecular interaction at the air/aqueous or air/solid interfaces, as indicated by their β_{SL}^{σ} and β_{LA}^{σ} values, and enhanced adsorption of the surfactant mixture at the solid substrate/solution interface relative to that at the air/solution interface, as shown in Figure 1. In our current investigation, the relationship between synergistic spreading, adsorption enhancement, molecular interaction, and dynamic contact angles, all from mixed surfactant solutions, has been studied for mixtures of hydrocarbon-chain surfactants. For convenience of comparison, in all the surfactant mixtures studied, the mole fractions of the component (α) in the mixed solutions (on a surfactant-only basis) used for the study of adsorption, molecular interactions, and dynamic contact angles, have been picked according to the condition that produces maximal spreading enhancement from the mixed surfactant solutions. The greatly enhanced spreading observed with certain of these hydrocarbon-chain mixtures is the subject of a recent patent application.[17]

Experimental Procedures

Materials. The structures of some of the studied surfactants are shown in Scheme 1A. *n*-C_8H_{17}-*N*-pyrrolidone (C8P) and *n*-$C_{12}H_{25}$-*N*-pyrrolidone (C12P) were supplied by ISP Technologies, Inc. (Wayne, NJ), Igepal CA-520 was supplied by Rhodia (Cranbury, NJ). All were used without further purification. *n*-$C_4H_9OPhSO_3Na$ was synthesized previously in our laboratory. PE powder was supplied by U.S.I. Chemicals (Cincinnati, OH), with a specific area of 0.36 m^2/g.

Sodium chloride used to increase the ionic strength and provide a constant counterion concentration in the aqueous surfactant solution was reagent-grade material that had been baked for at least 5 h in a porcelain casserole at red heat to burn and remove traces of organic compounds. The surface tension of the aqueous solution of the baked salt was measured, to ensure the absence of traces of surface-active impurities.

Surface Tension Measurements. Measurements were performed at 25 °C with a torsion balance by the Wilhelmy vertical technique, using a sand-blasted platinum plate of ~5 cm perimeter. The solutions were immersed in a constant-temperature bath at the desired temperature ±0.05 °C. The instrument was calibrated against quartz-condensed, double-distilled water (the last distillation stage from alkaline permanganate through a 1-m-high Vigreaux column with quartz condenser and receiver), every day that measurements were made. Sets of measurement were taken at certain intervals until the surface tension was constant for ~0.5 h. The standard deviation for surface tension measurements was less than 0.2 mN/m.

Adsorption of Surfactant on PE Powder. PE powder was cleaned by washing at least eight times with spectranalyzed methanol and then dried in a vacuum desiccator over anhydrous phosphorus pentoxide (P_2O_5) for a few weeks. A series of surfactant solutions (25−40 mL) are mixed with the appropriate amount of purified PE powder (0.5−1.0 g). Vigorous overnight shaking at room temperature was carried out on the mixtures to ensure adsorption equilibrium. The mixture was centrifuged to separate the powder from the surfactant solution. For all the studied surfactant solutions, both the individual and mixed surfactant solutions, the equilibrium surfactant concentrations were measured by UV absorbance against corresponding calibration curves. Adsorption amount at the corresponding equilibrium concentration was calculated from the surfactant concentration difference before and after adsorption.

Surfactant Concentration Measurement by UV Absorbance. The equilibrium concentrations of surfactants were determined by measuring their UV absorbance (UV/Vis spectrophotometer, HITACHI, U-2001). For the individual pyrroli-

(16) Wu, Y. F.; Rosen, M. J. *Langmuir* **2002**, *18*, 2205.
(17) U. S. Patent Application Serial No. 10/318, 321, Enhancement of the Wetting of Hydrophobic Surfaces by Aqueous Surfactant Solutions.

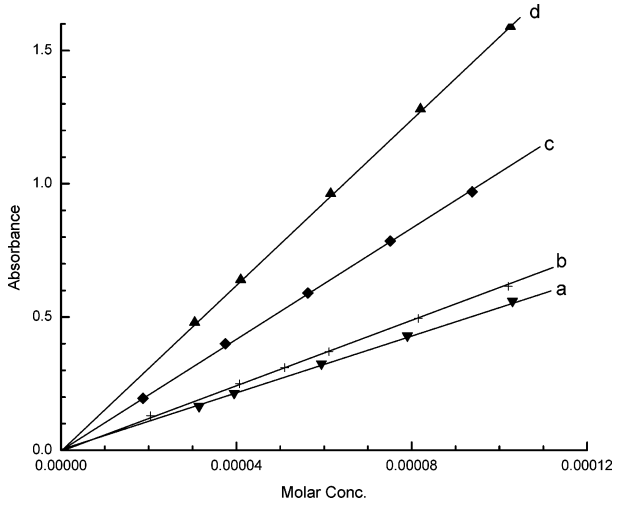

Figure 2. Absorbance calibration curves for studied surfactants at different wavelengths: (a) absorbance of C12P at $\lambda = 205$ nm; (b) absorbance of C8P at $\lambda = 205$ nm; (c) absorbance of CA-520 at $\lambda = 223$ nm; (d) absorbance of *n*-$C_4H_9OPhSO_3Na$ at $\lambda = 233$ nm.

done surfactant solutions (C8P and C12P), even though they do not have a maximal wavelength in the UV−vis range, their UV absorbances still obey Beer's law, as shown in Figure 2. Both CA-520 and *n*-$C_4H_9OPhSO_3Na$ show maximal UV absorbance due to the presence of the aromatic ring. For the binary mixed surfactant solution, according to Beer's law, the total absorbance of the solution is given by $A_{total} = A_1 + A_2 = \epsilon_1 bC_1 + \epsilon_2 bC_2$. When the concentration of one component is determined by UV absorbance, the contribution from the other must be deducted.

Dynamic Contact Angle Measurements on PE Film. Dynamic advancing contact angles were measured with a contact angle image analysis system (model 100-00, Ramé-hart, Inc.). One drop of surfactant solution, around 10 μL, was applied to the PE film (prepared as described below), which was placed in a thermostatic environmental chamber (model 100-07, Ramé-hart, Inc.) saturated with solvent vapor to retard droplet evaporation. Angles were measured on both sides of the drop at 25 °C. The measurement of dynamic contact angles is started as soon as possible, usually less than 10 s after the solution drop has been placed on the solid substrate, and is continued for the first 180 s. The average of at least three measurements was taken for the reading. The observed contact angle of H_2O on this kind of film is from 95° to 100°.

Spreading Factor Measurements. PE film was made by carefully melting PE powder (purified as described above) on a 10 cm × 10 cm dry clean glass square and then removing it after the film has solidified. To remove the entire PE film from the glass safely, the removing process has to be performed in boiling distilled water. The side of the PE film that had contacted the glass (which was much smoother than the other side) was used for measuring the spreading factor. PE film was mounted horizontally on an optically flat glass plate. By use of a microsyringe, which had previously been rinsed with the solution being tested, a 20 μL drop of the solution was placed on the PE film. Then another 10 cm × 10 cm glass square was immediately placed above the PE film. After 3 min (when the solution had stopped spreading), an outline of the spread solution was traced onto the top glass. This area was then retraced onto standard white paper from which it was cut and weighed. The exact spreading area was then calculated from the mass of a piece of the same paper of known area, with the assumption that the paper has a constant mass per unit area.

After each measurement, the PE substrate was thoroughly rinsed with methanol, tap water, and distilled water and was then put into boiling distilled water for at least 30 min to remove any adsorbed surfactant. Each spreading measurement was done three to five times until reproducibility was satisfactory. The spreading area is the average of the areas obtained in each set of measurements. The spreading factor (SF) is the ratio of spreading area of the surfactant solution to spreading area of the same volume of solvent in the same time (3 min).

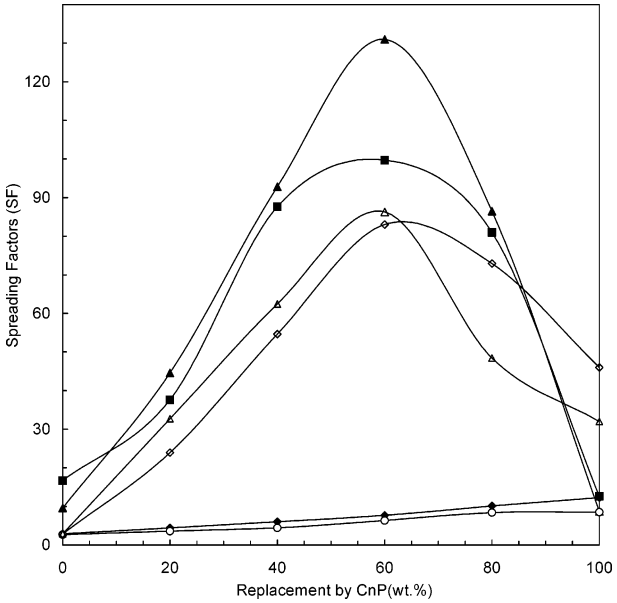

Figure 3. Effect of C*n*P replacement on spreading factors for some surfactant mixture systems on purified PE film, total surfactant concentration of the solution is 1.0 g/L: (▲) C8P/CA-520 system in 0.1 M NaCl medium; (■) C8P/CA-520 system in H_2O; (△) C12P/*n*-$C_4H_9OPhSO_3Na$ system in 0.1 M NaCl medium; (◇) C12P/*n*-$C_4H_9OPhSO_3Na$ system in H_2O; (◆) C8P/*n*-$C_4H_9OPhSO_3Na$ system in H_2O; (○) C8P/*n*-$C_4H_9OPhSO_3Na$ system in 0.1 M NaCl.

Results and Discussion

Spreading on Purified PE Film. Figure 3 shows the spreading results of some aqueous surfactant solutions on purified PE film, for both individual and mixed surfactant solutions. The mixed solutions of surfactant CA-520 and C8P show better spreading on purified PE film than either individual component in both H_2O and 0.1 M NaCl media. The maximal spreading enhancement occurs when there is ca. 60% (wt %) replacement by C8P in the mixed surfactant solution, with larger enhancement from the mixed surfactant solution in 0.1 M NaCl medium. On the other hand, no synergistic spreading is observed for the mixed solution of C8P/*n*-$C_4H_9OPhSO_3Na$. Also shown in Figure 3 is the effect of C12P replacement on spreading enhancement from the mixed solution of C12P/*n*-$C_4H_9OPhSO_3Na$ in both H_2O and 0.1 M NaCl media. Maximal spreading enhancement in this system again occurs when there is ca. 60% (wt %) replacement by C12P in the mixture solution, with somewhat larger enhancement from the mixed solution in 0.1 M NaCl medium. The maximal spreading performance from mixed solution of C8P/CA-520 on purified PE film, with a SF value of 130, is almost the same as the so-called superspreading normally obtainable from trisiloxane surfactants (SF value of 150).

Adsorption Enhancement from Mixed Solutions. Figure 4A shows the difference between adsorption of the individual surfactants from their solutions and from their mixed surfactant solutions for the C8P/CA-520 system in 0.1 M NaCl medium, with fixed initial α values (all α values shown in subsequent figures are fixed initial values). Clearly, C8P has a higher adsorption from a pure C8P surfactant solution than from the mixed surfactant solution. But CA-520 in the mixture shows a substantial increase in adsorption compared to that from a pure CA-520 surfactant solution. Since CA-520 contributes

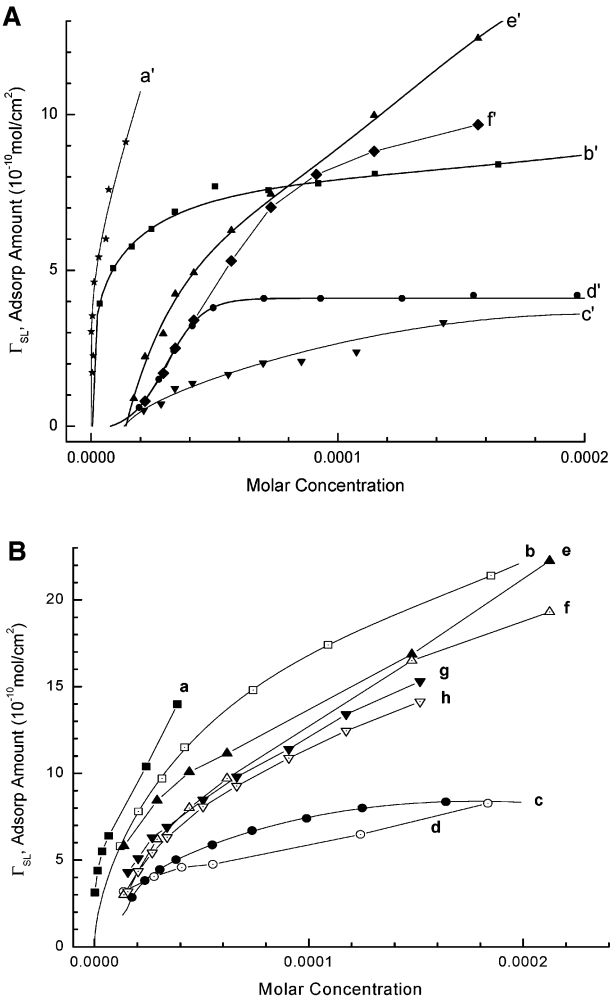

Figure 4. (A) In 0.1 M NaCl medium, increased adsorption of CA-520 from the C8P/CA-520 mixture (a′) than from a pure CA-520 solution (b′); decreased adsorption of C8P from the C8P/CA-520 mixture (c′) than from a pure C8P solution (d′); and increased adsorption from the C8P/CA-520 mixture (e′), compared to its calculated ideal adsorption (**f′**), with initial $\alpha_{C8P} = 0.741$ in the mixture. (B) In H_2O medium, increased adsorption of CA-520 from the C8P/CA-520 mixture (a) than from a pure solution (b); decreased adsorption of C8P from the C8P/CA-520 mixture (d) than from a pure solution (c); and increased adsorption from the C8P/CA-520 mixture (e and g) compared to its calculated ideal adsorption (f and h), with initial $\alpha_{C8P} = 0.684$ for plots e and f, initial $\alpha_{C8P} = 0.761$ for plots g and h.

much more than C8P to the total adsorption from the C8P/CA-520 mixture solution under the conditions of this study, the observed adsorption from the C8P/CA-520 mixture is higher than its calculated ideal adsorption, as shown in Figure 4A. Here, the ideal adsorption of the mixture is the sum of the individual adsorptions of the two components obtained from their individual adsorption isotherms at the same individual bulk phase concentrations of the two components as in the mixture at that same initial α value.

The adsorption difference between the C8P/CA-520 mixed solution and its individual components in H_2O is almost the same as that observed in 0.1 M NaCl medium. Again, there is stronger adsorption of C8P from pure C8P solution than from the mixture, but stronger adsorption of CA-520 from the mixture than from the pure CA-520 solution. Also, the resulting total adsorption from the C8P/CA-520 mixture in H_2O is higher than its calculated ideal adsorption, as shown in Figure 4B. The observed

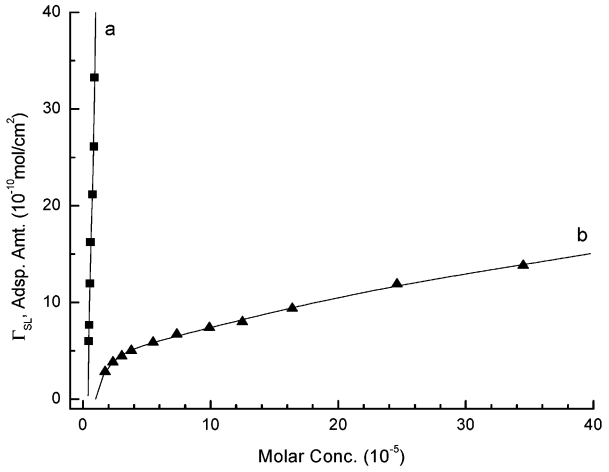

Figure 5. Comparison of the adsorptions of C8P and C12P in H_2O. **a**: C12P; **b**: C8P.

increase in the adsorption after mixing CA-520 and C8P surfactants does not change with the medium change from 0.1 M NaCl to H_2O, except that greater adsorption is observed in the latter medium.

Compared to the adsorption of C8P in H_2O, C8P shows a substantial decrease in adsorption amount onto purified PE powder in 0.1 M NaCl medium. Calculated A_{min} (area per molecule) values indicate that there is monolayer adsorption formation on hydrophobic PE powder in 0.1 M NaCl medium but multilayer adsorption formation on PE powder in H_2O. The decreased adsorption and monolayer formation on PE powder have also been observed in phosphate buffer medium.[18] The decrease of the adsorption in high ionic strength medium may be ascribed to the stabilization of the ionic resonance structure of C8P by the NaCl in the solution, as shown in Scheme 1B. Since ionic surfactants usually show monolayer adsorption onto nonpolar hydrophobic surfaces, ionic-like C8P surfactant in high ionic strength medium presumably results in the monolayer adsorption.

Compared to C8P, the individual C12P solution has a much higher adsorption (Figure 5), because of the longer hydrophobic alkyl chain and its limited solubility in aqueous solution. Even in the C12P/*n*-$C_4H_9OPhSO_3Na$ mixture solution, where C12P can be completely dissolved, it still shows very high adsorption ability. Because of its extraordinary strong adsorption ability, there is no apparent difference between the adsorption of C12P from a pure solution and from the C12P/*n*-$C_4H_9OPhSO_3Na$ mixed solution. On the other hand, in the presence of C12P, *n*-$C_4H_9OPhSO_3Na$ in the mixture shows much higher adsorption than that from a pure *n*-$C_4H_9OPhSO_3Na$ solution in both H_2O and 0.1 M NaCl media (Figure 6A). Also the observed total adsorptions from the C12P/*n*-$C_4H_9OPhSO_3Na$ solutions are higher than the correspondingly calculated ideal adsorptions from the mixture, as shown in Figure 6B. Corresponding to the spreading results of the C8/*n*-$C_4H_9OPhSO_3Na$ mixture in Figure 3, no adsorption enhancement has been observed from this mixture, compared to its calculated total ideal adsorption. And both components showed a lower adsorption from the mixed surfactant solution than from their pure surfactant solutions.

Molecular Interactions at the Solid/Aqueous Solution Interface. To gain insights into the reason for the adsorption results described above, surfactant molecular interactions at the purified PE powder/aqueous solution

(18) Rosen, M. J.; Wu, Y. F. *Langmuir* **2001**, *17*, 7296.

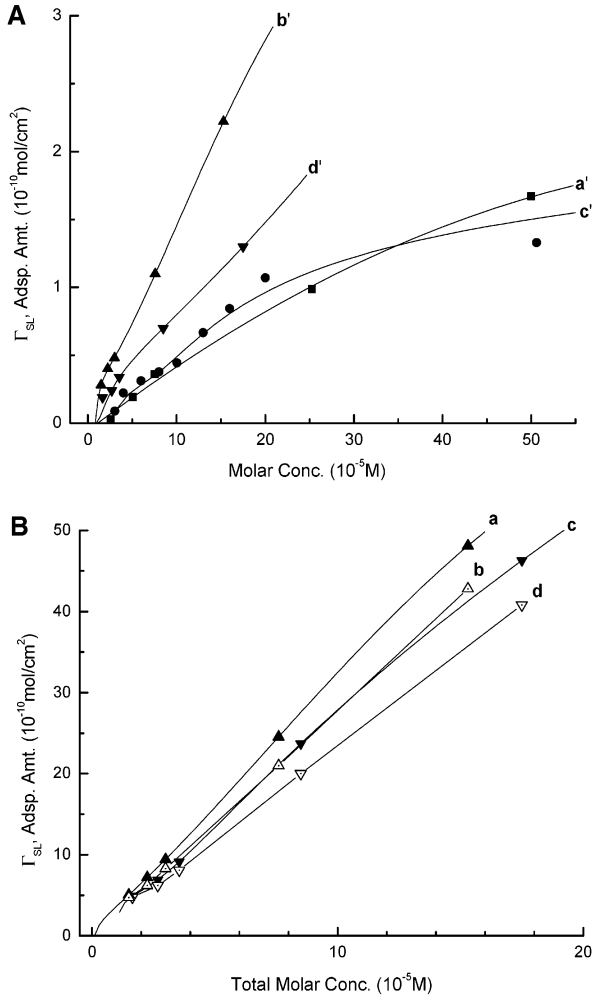

Figure 6. (A) Increased adsorption of *n*-$C_4H_9OPhSO_3Na$ from the C12P/*n*-$C_4H_9OPhSO_3Na$ mixture (b′) than from a pure *n*-$C_4H_9OPhSO_3Na$ solution (a′) in 0.1 M NaCl. Also increased adsorption of *n*-$C_4H_9OPhSO_3Na$ from the C12P/*n*-$C_4H_9OPhSO_3Na$ mixture (d′) than from a pure *n*-C_4H_9-$OPhSO_3Na$ solution (c′) in H_2O. (B) Increased adsorption of the C12P/*n*-$C_4H_9OPhSO_3Na$ mixture (a), compared to its calculated ideal adsorption (b) in 0.1 M NaCl; and increased adsorption of the C12P/*n*-$C_4H_9OPhSO_3Na$ mixture (c), compared to its calculated ideal adsorption (d) in H_2O, with initial $\alpha_{C12P} = 0.604$ in both mixtures.

interface have been studied. The calculation of interaction parameters at this solid/aqueous solution interface involves direct measurement of surfactant adsorption isotherms instead of interfacial tensions.

The interfacial pressure of a system, designated π, measures the difference between the interfacial tension of the pure solvent (e.g., H_2O), γ^0, and the interfacial tension of the surfactant solution, γ. Thus

$$\pi_{SL} = \gamma_{SL}{}^0 - \gamma_{SL} \tag{1}$$

where γ_{SL} is the interfacial tension of a surfactant solution at the solid/liquid interface and $\gamma^0{}_{SL}$ is the interfacial tension between the pure solvent (e.g., H_2O) and the solid at the solid/liquid interface. From surfactant adsorption isotherms, interfacial pressure at solid/liquid interface can be calculated as[16]

$$\pi_{SL} = RT \int_0^C \Gamma_{SL}\, \mathrm{d} \ln C \tag{2}$$

where Γ_{SL} is the adsorption of the surfactant at the solid/liquid interface, in mol/cm^2; C is the concentration of surfactant in bulk solution phase below the critical micelle concentration (cmc) in mol/L; T is temperature of the system, in K; and R is the gas constant of 8.314 J·mol^{-1}·K^{-1}.

Equation 2 can be used both for individual surfactant solutions (eq 3) and for two-component mixed surfactant systems, 1 + 2 (eq 4)

$$\pi_{SL}{}^1 = RT \int_0^{C_A} \Gamma_{SL}{}^A\, \mathrm{d} \ln C_A \tag{3}$$

$$\pi_{SL}{}^{Mix} = RT \int_0^{C_{Total}} \Gamma_{SL}{}^{Total}\, \mathrm{d} \ln C_{total} \tag{4}$$

where $\pi_{SL}{}^1$ is the interfacial pressure at the solid/liquid interface caused by the solution of component 1, C_1 is the concentration of the component 1 in the bulk solution by itself, and $\Gamma_{SL}{}^1$ is the adsorption of the component 1 at the solid/liquid interface. Similarly, $\pi_{SL}{}^{Mix}$ is the interfacial pressure at the solid/liquid interface caused by the mixed solution of 1 and 2, C_{total} is the total concentration of the surfactant mixture in the bulk solution, and $\Gamma_{SL}{}^{Total}$ is the total adsorption of the surfactant mixture at the solid/liquid interface. The values of Γ_{SL} for use of eqs 3 and 4 are obtained from adsorption isotherms of individual surfactants or mixtures of surfactants. A plot of Γ_{SL} vs ln C is integrated to obtain π_{SL} as a function of ln C. π_{SL} is then plotted as a function of ln C for both individual surfactant components and their mixture at a given value of α_1, the mole fraction of surfactant 1 (on a surfactant-only basis), as illustrated later in Figure 8. The interaction parameters at the PE powder/aqueous solution interface, $\beta_{SL}{}^{\sigma}$, are then calculated from these plots, by using the following equation[15b]

$$\frac{X_1{}^2 \ln(\alpha_1 C_{12}/X_1 C_1{}^0)}{(1 - X_1)^2 \ln[(1 - \alpha_1)C_{12}/(1 - X_1)C_2{}^0]} = 1 \tag{5}$$

$$\beta^{\sigma} = \frac{\ln(\alpha_1 C_{12}/X_1 C_1{}^0)}{(1 - X_1)^2} \tag{6}$$

where X_1 is the molar fraction of surfactant 1 in the mixed monolayer at the solid/liquid interface (on a surfactant-only basis), $C_1{}^0$, $C_2{}^0$, and C_{12} are the molar concentrations of surfactant 1, surfactant 2, and their mixture, respectively, required to produce the same value of π_{SL}, and α_1 is the molar fraction of surfactant 1 in the solution phase (on a surfactant-only basis) at adsorption equilibrium. Equation 5 is solved numerically for X_1, which is then substituted into eq 6 to calculate β^{σ}. Equations 5 and 6 are also used to calculate β values at the air/aqueous solution interface ($\beta_{LA}{}^{\sigma}$), where $C_1{}^0$, $C_2{}^0$, and C_{12} are the molar concentrations of surfactant 1, surfactant 2, and their mixture, respectively, required to produce a given surface tension, γ, value.

Figure 7 shows the adsorption isotherms of both the individual nonionic surfactants CA-520, C8P, and their mixtures in H_2O. From their adsorption isotherms, $\Gamma_{SL}{}^{Total}$ and $\Gamma_{SL}{}^{C8P}$ can be plotted as a function of ln C_{total} and ln C_{C8P}, respectively. From these, $\pi_{SL}{}^{Mix}$ and $\pi_{SL}{}^{C8P}$ can be calculated from the integration of plots of $\Gamma_{SL}{}^{Total}$ vs ln C_{total} and $\Gamma_{SL}{}^{C8P}$ vs ln C_{C8P} (eqs 4 and 3, respectively). The definite integrals in eqs 3 and 4 are just the areas under the plots of Γ vs ln C from C equal 0 to C. (Area integrals are calculated from the fitting equations obtained by use of Origin 6.0.) Figure 8 shows the plots of the calculated interfacial pressure, π_{SL}, at the purified PE powder/

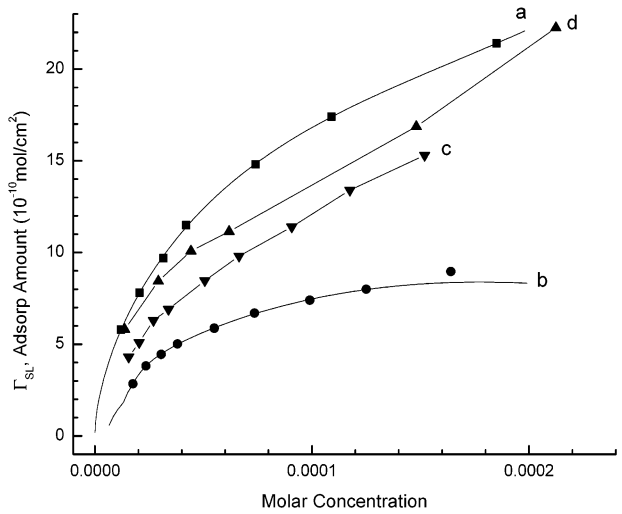

Figure 7. Adsorption isotherms of C8P, Igepal CA-520, and their mixtures onto purified PE powder in H_2O: (a) individual CA-520; (b) individual C8P; (c) C8P/CA-520 mixture with $\alpha_{C8P} = 0.761$; (d) C8P/CA-520 mixture with $\alpha_{C8P} = 0.684$.

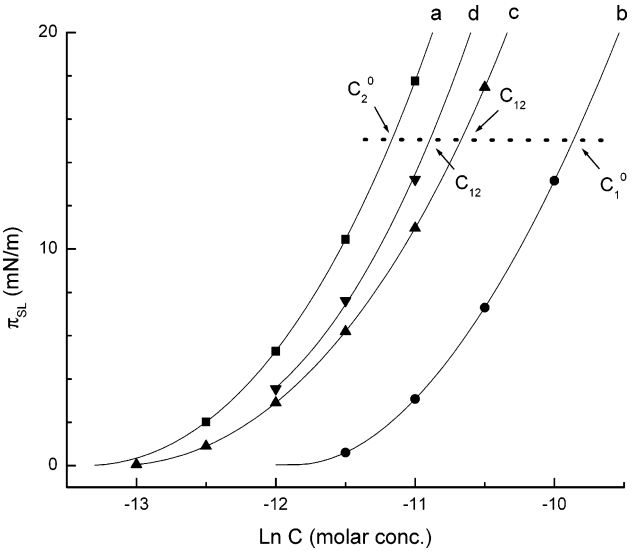

Figure 8. Plots of interfacial pressure, π_{SL}, at purified PE powder/aqueous solution interface vs ln C for C8P, CA-520, and their mixtures in H_2O (concentration, C, in mol/L): (a) individual CA-520; (b) individual C8P; (c) C8P/CA-520 mixture with $\alpha_{C8P} = 0.761$; (d) C8P/CA-520 mixture with $\alpha_{C8P} = 0.684$.

aqueous solution interface vs ln C for both individual surfactants and their mixtures. These plots are used for the calculation of β parameters.

Unlike the calculation of $\beta_{LA}{}^{\sigma}$ at the air/aqueous solution interface, where concentration values of $C_1{}^0$, $C_2{}^0$, and C_{12} in eq 5, corresponding to the lowest possible common surface tension in both individual and mixed solutions are used, concentration values for the $\beta_{SL}{}^{\sigma}$ calculation corresponding only to the highest common value of π_{SL} below the monolayer can be used, as shown in Figure 8. This is because the equations for calculating $\beta_{SL}{}^{\sigma}$ are based upon the Gibbs adsorption equation and are consequently only valid for monolayers. The value of α_{C8P}, the molar fraction of C8P in the bulk solution phase at adsorption equilibrium, is generally not equal to the initial value, due to the different adsorption ability of the two individual surfactants onto purified PE powder. The experimental equilibrium values of α_{C8P} are calculated by finding the bulk concentrations of both components in the mixed solution, which is achieved by UV−vis spectroscopy. Then

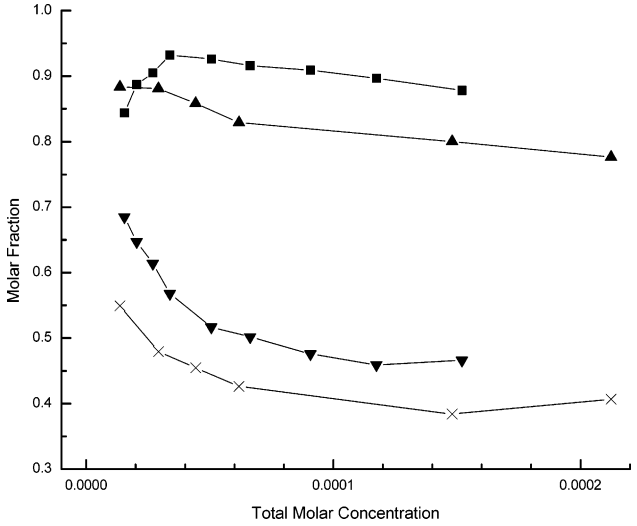

Figure 9. Plots of the molar fraction of C8P (α_{C8P}) in the bulk solution phase and the molar fraction of C8P (X_{C8P}) at the solid/aqueous solution interface at adsorption equilibrium vs total mixture concentration at different fixed initial molar fractions of C8P in the bulk solution of C8P/CA-520 mixtures in H_2O: (■) α_{C8P} with initial fixed $\alpha_{C8P} = 0.761$; (▲) α_{C8P} with initial fixed $\alpha_{C8P} = 0.684$; (▼) X_{C8P} with initial fixed $\alpha_{C8P} = 0.761$; (×) X_{C8P} with initial fixed $\alpha_{C8P} = 0.684$.

experimental equilibrium values of X_{C8P}, the molar fraction of C8P at solid/aqueous solution interface at adsorption equilibrium, are calculated from the concentration difference before and after surfactant adsorption. The variations of calculated α_{C8P} and X_{C8P} values with equilibrium concentration change of the surfactant mixture solution are shown in Figure 9. Since CA-520 is more strongly adsorbed onto PE powder than C8P (Figure 7), substantial increases in the values of α_{C8P} are observed after surfactant adsorption from the mixed solutions.

Tables 1 lists the calculated $\beta_{SL}{}^{\sigma}$ values for the two C8P/CA-520 mixtures studied in H_2O. All the β parameters calculated under the studied interfacial pressures are negative, indicating a net attractive interaction at the PE powder/aqueous solution interface after mixing of the two surfactants. Interaction parameters at the air/aqueous solution interface ($\beta_{LA}{}^{\sigma}$) for the C8P/CA-520 mixture in H_2O have also been calculated. The corresponding surface tension plots for the individual surfactants and their mixtures are shown in Figure 10, and the calculated β parameters at the air/aqueous solution interface are listed in Table 2. From Table 2, only small negative $\beta_{LA}{}^{\sigma}$ values resulted after mixing of the two surfactants, C8P and CA-520, in H_2O, which indicate an almost ideal mixing behavior at the air/aqueous solution interface.

On comparison of the values of $\beta_{SL}{}^{\sigma}$ and $\beta_{LA}{}^{\sigma}$, it is clear that significantly negative β parameters are obtained only at the PE powder/aqueous solution interface. The strength of the surfactant molecular interaction at the PE powder/aqueous solution interface, as indicated by the absolute value of $\beta_{SL}{}^{\sigma}$, is related to the adsorption performance of the surfactant mixture at the solid/aqueous solution interface. The significantly attractive interaction at the PE powder/aqueous solution interface after mixing, compared to the weak molecular interaction occurring at the air/aqueous solution interface, results in spreading enhancement with the C8P/CA-520 mixtures.

The same study has been performed for the C8P/CA-520 system in 0.1 M NaCl medium. Adsorption isotherms of the surfactants C8P, CA-520, and their mixtures in 0.1 M NaCl have been measured, then the corresponding plots of adsorption vs ln C and interfacial

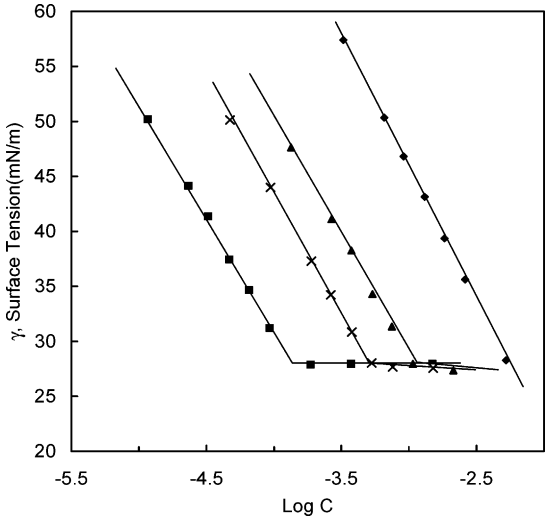

Figure 10. Plots of the surface tension, γ, vs log C (bulk phase concentration) for C8P, CA-520, and their mixtures in H_2O: (■) CA-520; (×) C8P/CA-520 mixture with initial $\alpha_{C8P} = 0.763$; (▲) C8P/CA-520 mixture with initial $\alpha_{C8P} = 0.900$; (◆) C8P.

Table 1. Interaction Parameters at the Purified PE Powder/Aqueous Solution Interface for the C8P/CA-520 Mixture in H_2O

initial α_{C8P}	0.761	0.684
equilibrium α_{C8P}	0.89	0.88
calculated X_{C8P}	0.59	0.57
experimental X_{C8P}	0.63	0.54
β_{SL}^{σ}	−2.38	−3.15
A_{min} of CA-520[a]	27	27
A_{min} of mixture[a]	27	23
A_{min} of C8P[a]	29	29

[a] A_{min}: area/molecule at the solid/liquid interface under the concentration used for β calculation, in units of Å^2.

Table 2. Interaction Parameters at the Air/Aqueous Solution Interface for the C8P/CA-520 Mixture in H_2O

α_{C8P}	0.900	0.763
β_{LA}^{σ}	−0.25	−0.24
X_{C8P}	0.20	0.09
A_{min} of CA-520[a]	43.5	43.5
A_{min} of mixture[a]	42	43
A_{min} of C8P[a]	38.5	38.5

[a] A_{min}: area/molecule at the air/aqueous interface under the concentration used for β calculation, in unit of Å^2.

pressure (π_{SL}) vs ln C for both individual and mixtures have been determined. In 0.1 M NaCl medium, the C8P/CA-520 mixture solution also shows stronger adsorption than either of the individual component surfactants onto purified PE powder, and fairly negative β_{SL}^{σ} values have been observed at the PE powder/aqueous solution interface. Again, the significantly attractive interaction at the solid/aqueous solution interface after mixing, compared to the weak molecular interaction occurring at the air/aqueous solution interface, accounts for the spreading enhancement from the C8P/CA-520 mixtures.

The calculation of the interaction parameters at the purified PE powder/aqueous solution interface (β_{SL}^{σ}) has also been performed for some other systems. Adsorption isotherms of the surfactants C12P, *n*-$C_4H_9OPhSO_3Na$, and their mixtures in both 0.1 M NaCl and H_2O media have been measured, then the corresponding plots of adsorption vs ln C and interfacial pressure (π_{SL}) vs ln C for both individual and mixtures, which is used for the calculation of β_{SL}^{σ}, have been determined. Table 3 shows the interaction parameters at the purified PE powder/aqueous solution interface (β_{SL}^{σ}) for C12P/*n*-$C_4H_9OPhSO_3Na$ mixtures in both 0.1 M NaCl and H_2O media. Negative interaction parameters (β_{SL}^{σ}) are observed at the PE powder/aqueous solution interface in C12P/*n*-$C_4H_9OPhSO_3Na$ mixtures, both in 0.1 M NaCl and in H_2O media. Also, as in the C8P/CA-520 mixtures, strong attractive interaction after mixing C12P and *n*-$C_4H_9OPhSO_3Na$ only occurred at the PE powder/aqueous solution interface, and weak surfactant molecular interactions were observed at the air/aqueous solution interface. The significantly attractive interaction at the PE powder/aqueous solution interface after mixing, compared to the weak interaction at the air/aqueous solution interface, results in spreading enhancement in the mixtures.

Table 3. Interaction Parameters at Purified PE Powder/Aqueous Solution Interface for CnP/*n*-$C_4H_9OPhSO_3Na$ Mixture, with Fixed Initial α_{CnP}

CnP	initial α_{CnP}	medium	equilibium α_{CnP}	equilibium X_{CnP}	β_{SL}^{σ}	β_{LA}^{σ}
C12P	0.604	H_2O	0.20	0.72	−4.4	−0.40
	0.604	0.1 M NaCl	0.25	0.73	−4.5	−0.42
C8P	0.572	H_2O	0.47	0.96	>1	−0.20
	0.570	0.1 M NaCl	0.56	0.69	>1	−0.32

Table 3 also shows the interaction parameters at the purified PE powder/aqueous solution interface (β_{SL}^{σ}) for C8P/*n*-$C_4H_9OPhSO_3Na$ mixtures in both 0.1 M NaCl and H_2O media. The adsorption isotherms for surfactants C8P, *n*-$C_4H_9OPhSO_3Na$, and their mixtures and the corresponding plots of adsorption vs ln C and interfacial pressure (π) vs ln C for both individual and mixtures have been determined. Again, small negative β parameters (β_{LA}^{σ}) indicating weak molecular interactions at the air/aqueous solution interface were obtained. However, in contrast to C12P/*n*-$C_4H_9OPhSO_3Na$ and C8P/CA-520 mixtures, no significantly negative interaction parameters at the PE powder/aqueous solution interface (β_{SL}^{σ}) were obtained, and no adsorption enhancement and no spreading enhancement were observed with the C8P/*n*-$C_4H_9OPhSO_3Na$ mixtures.

Dynamic Contact Angles. As mentioned earlier, spreading is a dynamic process, so dynamic contact angles instead of equilibrium contact angles of aqueous solutions on hydrophobic PE substrate have been studied. Like equilibrium contact angles, dynamic contact angles also indicate the hydrophobic/hydrophilic property of the solid. High contact angles against water mean a hydrophobic surface of the solid. Lower contact angles against water can be achieved through modification of the hydrophobic surface of the solid by surfactant adsorption at the solid/liquid interface with their hydrophilic headgroups oriented toward the aqueous phase. Therefore, the observed contact angle indicates the adsorption ability and orientation of the surfactant onto the hydrophobic surface of the solid substrate.

Figure 11A shows the observed dynamic contact angle measurements of the surfactant solutions C8P, CA-520, and their mixture in H_2O, with the surfactant component concentration in the mixture the same as its concentration in its pure solution. The measurement is taken every 15 s for the first 3 min after the solution drop has just been settled on the purified PE film. Lower dynamic contact angles were observed for the C8P/CA-520 mixture solution than for the solution of either of the individual components. The lower the dynamic contact angle as a function of time, the faster adsorption is occurring at the interfaces and probably the greater the surfactant concentration and surface tension gradients in the precursor film of the solution droplet. For hydrocarbon chain surfactants,

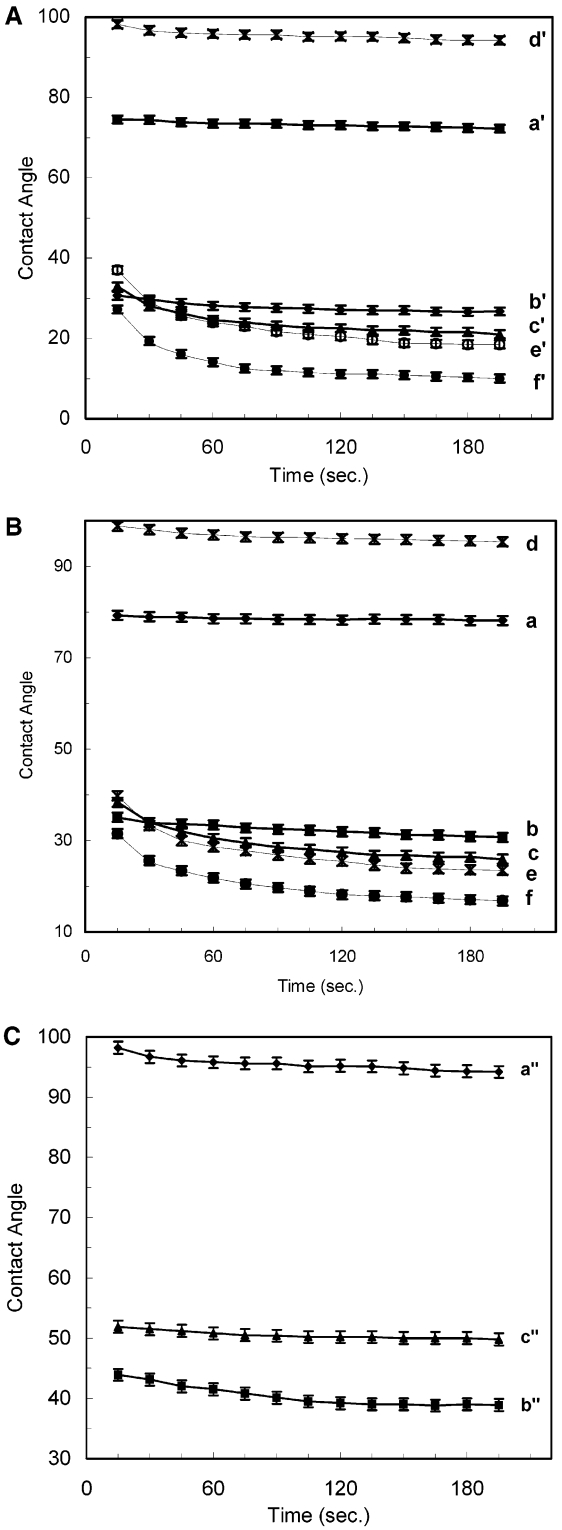

Figure 11. Dynamic contact angles of the surfactants and their mixtures. (A) In H_2O medium: (a′) 0.05 g/L of C8P; (b′) 0.05 g/L of CA-520; (c′) 0.1 g/L of C8P/CA-520 mixture, 50% (wt %) each; (d′) 0.1 g/L of *n*-$C_4H_9OPhSO_3Na$; (e′) 0.1 g/L of C12P; (f′) 0.2 g/L of C12P/*n*-$C_4H_9OPhSO_3Na$ mixture, 50% (wt %) each. (B) In 0.1 M NaCl: (a) 0.05 g/L of C8P; (b) 0.05 g/L of CA-520; (c) 0.1 g/L of C8P/CA-520 mixture, 50% (wt %) each; (d) 0.1 g/L of *n*-$C_4H_9OPhSO_3Na$; (e) 0.1 g/L of C12P; (f) 0.2 g/L of C12P/*n*-$C_4H_9OPhSO_3Na$ mixture, 50% (wt %) each. (C) Dynamic contact angles of the surfactant solutions C8P, *n*-$C_4H_9OPhSO_3Na$ and their mixture in H_2O: (a″) 0.5 g/L of *n*-$C_4H_9OPhSO_3Na$; (b″) 0.5 g/L of C8P; (c″) 1.0 g/L of C8P/*n*-$C_4H_9OPhSO_3Na$ mixture, 50% (wt %) each. Slightly higher dynamic contact angles for both the pure components and the mixture were observed in 0.1 M NaCl medium.

adsorption at the solid/air interface has been shown to be at least 1 order of magnitude smaller than those at the solid/aqueous solution and air/aqueous solution interfaces.[18] We have also shown that adsorption of C8P onto purified PE powder at the solid/aqueous solution interface, is much greater than its adsorption at the air/aqueous solution interface. The observed lower contact angles for the C8P/CA-520 mixture are consistent with the observed adsorption enhancement in C8P/CA-520 mixture at the solid/aqueous solution interface (Figure 4). The lower dynamic contact angles indicate faster adsorption, which should generate a larger concentration difference between solutions in the precursor film and bulk solutions in the droplet than either of the component surfactants. Consequently, the spreading coefficient at the solid/liquid interface ($S_{L/S}$) for the C8P/CA-520 mixture, defined as $S_{L/S} = \gamma_{SA} - (\gamma_{SL} + \gamma_{LA})$, will increase, compared to its individual components C8P and CA-520, because of the major decrease in γ_{SL}, which results from the enhanced adsorption from the mixture at the solid/aqueous solution interface. Therefore, the observed lower dynamic contact angles from the C8P/CA-520 mixture result in spreading enhancement on PE film, as shown in Figure 3. Starov et al. also reported that surfactant adsorption onto the solid hydrophobic substrate controls the rate of spreading, ascribed to the hydrophilization of the initially hydrophobic solid surface by adsorbed surfactant molecules.[19]

Lower dynamic contact angles have also been observed for the C8P/CA-520 mixture in 0.1 M NaCl and the C12P/*n*-$C_4H_9OPhSO_3Na$ mixtures in both H_2O and 0.1 M NaCl than for either of the components in the mixture, as shown in parts A and B of Figure 11. And both adsorption enhancement and spreading enhancement have been observed in these mixtures. Once again, enhanced spreading after mixing of the two surfactants results from the major decrease in γ_{LS}, due to the observed adsorption enhancement at the solid/aqueous solution interface and the faster adsorption (as shown by the contact angles) after mixing.

Contrary to the C8P/CA-520 and C12P/*n*-$C_4H_9OPhSO_3Na$ mixtures, the C8P/*n*-$C_4H_9OPhSO_3Na$ mixture shows no spreading enhancement (Figure 3). Consistent with this, in Figure 11C, the dynamic contact angles of the C8P/*n*-$C_4H_9OPhSO_3Na$ mixture lie between those of the two components, in both H_2O and 0.1 M NaCl media. No enhancement in contact angle reduction is observed after mixing, and no adsorption enhancement has been observed for this mixture in either H_2O or 0.1 M NaCl medium. Those properties are between those of the two components. As a result, the spreading wetting ability of the C8P/*n*-$C_4H_9OPhSO_3Na$ mixture is between those of the two individual components.

Conclusions

Synergistic spreading on hydrophobic PE film has been observed in some of the pyrrolidone-containing mixed surfactant systems investigated. Spreading enhancement in the mixed surfactant systems is accompanied by stronger surfactant−surfactant attractive interactions and greater adsorption at the PE powder/aqueous solution interface than at the air/aqueous solution interface and by lower dynamic contact angles, implying greater dynamic spreading coefficients.

LA030157F

(19) Starov, V. M.; Kosvintsev, S. R.; Velarde, M. G. *J. Colloid Interface Sci.* **2000**, *227*, 185.